

# Evaluation of Topical Methotrexate in an Imiquimod-Induced Mouse Model of Psoriasis: Comparative Study with Clobetasol and Tacrolimus

Mohammed Abdul Muttalib Abdul Bari

Department of Pharmacy, Baghdad College of Medical Sciences, Baghdad 10001, Iraq

\*email: [Mohammedabdulmuttalibbari@gmail.com](mailto:Mohammedabdulmuttalibbari@gmail.com)

## Abstract

**Background:** Psoriasis is an immune-mediated skin disorder marked by abnormal keratinocyte proliferation and immune cell infiltration, with dysregulated cytokines such as TNF- $\alpha$ , IL-6, and IL-17. Methotrexate (MTX) is an established systemic therapy for moderate to severe psoriasis; however, the efficacy of topical MTX remains uncertain and requires further evaluation in controlled studies. **Purpose:** This study evaluated a 1% topical MTX formulation in an imiquimod-induced mouse model of psoriasis and compared its effects with topical clobetasol propionate (0.05%) and tacrolimus (0.1%). In addition, *in silico* molecular docking was performed as an exploratory complement to the clinical and histological assessments; docking results are hypothesis-generating and do not demonstrate direct *in vivo* mechanisms. The study did not include a systemic MTX arm. **Methods:** Male C57BL/6 mice were randomized into five groups (negative control, IMQ positive control, clobetasol, tacrolimus, and MTX 1%). Psoriasis-like dermatitis was induced with topical 5% imiquimod for 7 days, followed by twice-daily topical treatment for 14 days. Clinical severity was scored using a murine PASI scale; skin samples were collected for histopathology and for measurement of TNF- $\alpha$  and IL-6 by ELISA. *In silico* docking against TNF- $\alpha$  and IL-6 was performed using AutoDock Vina; docking is reported as exploratory. **Results:** Topical MTX produced marked reductions in PASI scores and improved histological architecture compared with IMQ controls, with effects comparable to clobetasol and greater than tacrolimus in this model. MTX-treated skin showed lower TNF- $\alpha$  and IL-6 levels (expressed as pg/mg protein). Docking simulations confirmed moderate predicted binding affinities of MTX, clobetasol, and tacrolimus to TNF- $\alpha$  and IL-6; these findings are presented as exploratory and hypothesis-generating, and do not constitute proof of direct cytokine binding *in vivo*. **Conclusion:** In this imiquimod mouse model, a 1% topical MTX formulation demonstrated significant anti-inflammatory and antiproliferative effects, comparable to topical clobetasol and superior to tacrolimus under the conditions tested. These results support further pharmacokinetic, skin penetration, and safety studies to confirm local bioavailability and to evaluate systemic exposure before clinical translation.

**Keywords:** psoriasis; methotrexate; clobetasol; tacrolimus; topical treatment; imiquimod model; TNF- $\alpha$ ; IL-6; molecular docking; cytokine modulation

**Citation:** Bari MAMA. Evaluation of Topical Methotrexate in an Imiquimod-Induced Mouse Model of Psoriasis: Comparative Study with Clobetasol and Tacrolimus. *Journal of Experimental Pharmacology and Toxicology* 2026;4. <https://doi.org/10.6425/042026jept005>

## 1. Introduction

Psoriasis is a chronic immune-mediated inflammatory skin disorder characterized by erythematous scaly plaques and markedly accelerated keratinocyte turnover. The condition arises from the interplay of genetic, environmental, and immunologic factors that drive abnormal keratinocyte proliferation and differentiation; whereas normal epidermal turnover is approximately 28 days, psoriatic epidermis renews in roughly 3–5 days, leading to accumulation of immature keratinocytes and thick scaling [1]. Clinically, psoriasis is recognized as a systemic inflammatory disease frequently associated with comorbidities such as psoriatic arthritis, cardiovascular disease, and metabolic syndrome, and it imposes a substantial symptom burden (pruritus, pain, fissuring) and reduced quality of life. Lesions commonly affect the scalp and extensor surfaces and may appear at sites of trauma (Koebner phenomenon) [1].

At the cellular and molecular level, innate and adaptive immune cells—including dendritic cells, macrophages, neutrophils, and T lymphocytes (notably Th1 and Th17 subsets)—orchestrate a cytokine-driven inflammatory cascade. The IL-23/IL-17 axis together with TNF- $\alpha$ , IL-6, and IFN- $\gamma$  are central mediators that promote keratinocyte hyperproliferation and sustain cutaneous inflammation; keratinocytes in turn amplify inflammation by releasing cytokines,

chemokines, and antimicrobial peptides [2]. These pathways underpin the rationale for targeted biologic and small-molecule therapies [1, 2].

Therapeutic goals are to reduce inflammation, normalize keratinocyte proliferation, relieve symptoms, and improve quality of life. For limited disease, topical agents (potent corticosteroids, vitamin D analogs, calcineurin inhibitors) remain first-line; clobetasol propionate is widely used for its strong anti-inflammatory and antiproliferative effects, while tacrolimus is an alternative in sensitive areas to avoid steroid-related atrophy [1]. For moderate to severe disease, systemic agents such as methotrexate (MTX) are effective; MTX acts as a folate antagonist inhibiting dihydrofolate reductase and related enzymes and increases extracellular adenosine, contributing to anti-inflammatory effects, but systemic MTX carries risks including hepatotoxicity and myelosuppression [3].

Topical MTX formulations aim to deliver local antiproliferative and anti-inflammatory activity while minimizing systemic exposure; however, topical delivery is challenging because MTX has low lipid solubility and a relatively high molecular weight that limit stratum corneum penetration, and prior clinical reports show inconsistent efficacy. These limitations motivate the development of optimized topical vehicles and preclinical evaluations of local bioavailability [3].

This study therefore evaluates a 1% topical MTX ointment in an imiquimod-induced mouse model of psoriasis, compares its effects with topical clobetasol propionate and tacrolimus, and uses exploratory *in silico* docking to generate mechanistic hypotheses that complement clinical and histological assessments.

## 2. Materials and Methods

### 2.1. Animals and Experimental Design

This study was conducted at the Center for Biotechnology, Al-Nahrain University. All experimental procedures followed standard laboratory practices for animal care and were conducted in accordance with internationally accepted guidelines (ARRIVE guidelines) to minimize animal suffering. All efforts were made to reduce the number of animals used and to ensure humane handling throughout the study.

A total of 48 male C57BL/6 mice (8–10 weeks old, 20–25 g) were randomly allocated into five groups using a computer-generated randomization table: negative control (no IMQ,  $n = 10$ ), positive control (IMQ only,  $n = 10$ ), IMQ + clobetasol 0.05% ( $n = 10$ ), IMQ + tacrolimus 0.1% ( $n = 9$ ), and IMQ + methotrexate 1% ( $n = 9$ ). Investigators performing clinical scoring and histological assessment were blinded to group allocation. All experiments were performed at the Center for Biotechnology, Al-Nahrain University.

### 2.2. Induction of Psoriasis-like Dermatitis and Topical Treatment

Psoriasis-like inflammation was induced by daily topical application of 5% imiquimod (IMQ) cream to the shaved dorsal skin for 7 consecutive days. Each mouse received 62.5 mg of 5% IMQ cream per day applied to a  $2 \times 3$  cm area. After the 7-day induction period, mice received topical treatments twice daily for 14 days as follows:

- Clobetasol propionate 0.05% ointment—50 mg/application (morning and evening).
- Tacrolimus 0.1% ointment—50 mg/application (morning and evening).
- Methotrexate 1% ointment—50 mg/application (morning and evening).

The MTX ointment vehicle used in this study was prepared as follows: white soft paraffin 70% w/w, liquid paraffin 20% w/w, propylene glycol 10% w/w, with methotrexate incorporated at 1% w/w. Formulations were prepared under aseptic conditions, homogenized by mechanical mixing, and stored at 4 °C in amber containers. Short-term homogeneity was confirmed by visual inspection and sampling.

### 2.3. Clinical Scoring (PASI)

Clinical severity was assessed daily using a murine PASI adapted scoring system evaluating erythema, induration (thickness), and scaling on a 0–4 scale (0 = none; 4 = very marked). The three component scores were summed to give a daily total (maximum 12). Scoring was performed independently by two blinded investigators and the mean of the two scores was used for analysis. PASI was recorded throughout the 7-day induction and the 14-day treatment periods [4].

### 2.4. Tissue Collection and Processing

At study end (day 21 from first IMQ application), animals were euthanized by CO<sub>2</sub> inhalation followed by cervical dislocation. Full-thickness dorsal skin samples were excised, weighed, and divided: one portion was fixed in 10% neutral

buffered formalin for histology; the remaining tissue was snap-frozen in liquid nitrogen and stored at  $-80^{\circ}\text{C}$  for biochemical assays.

## 2.5. Histopathology and Morphometry

Formalin-fixed tissues were processed, embedded in paraffin, and sectioned at  $5\ \mu\text{m}$ . Sections were stained with Hematoxylin and Eosin (H&E). A pathologist blinded to treatment scored histological features (inflammation, parakeratosis, epidermal thickness, vascular changes) using a standardized semiquantitative scale (0–3 for each feature). Epidermal thickness (basal layer to stratum granulosum) was measured morphometrically in ten random fields per section using ImageJ (NIH); the mean per animal was used for statistical analysis [5].

## 2.6. Cytokine Measurement (ELISA)

Approximately 50 mg of skin tissue was homogenized in 500  $\mu\text{L}$  of ice-cold phosphate-buffered saline (PBS) containing protease inhibitors using a tissue homogenizer. The homogenates were centrifuged at  $12,000 \times g$  for 15 min at  $4^{\circ}\text{C}$ , and the supernatants were collected and stored at  $-80^{\circ}\text{C}$  until analysis [6].

Tumor necrosis factor- $\alpha$  (TNF- $\alpha$ ) and interleukin-6 (IL-6) concentrations were measured using commercially available ELISA kits (R&D Systems, Minneapolis, MN, USA), Mouse TNF- $\alpha$  Quantikine ELISA Kit (Catalog No.: MTA00B) and Mouse IL-6 Quantikine ELISA Kit (Catalog No.: M6000B), following the manufacturer's instructions. Cytokine levels were expressed as pg/mg protein.

## 2.7. In Silico Molecular Docking

Target selection and preparation—selected protein targets and PDB IDs: DHFR (1U72), TYMS (1HVY), ATIC (1D3G), DHODH (6QU7), TNF- $\alpha$  (2AZ5), and IL-6 (1IL6). Protein structures were prepared by removing crystallographic waters, adding polar hydrogens, and assigning Kollman charges using AutoDock Tools. Ligands (methotrexate, clobetasol, tacrolimus) were energy-minimized using the MMFF94 force field in OpenBabel and converted to PDBQT format [7].

Molecular docking simulations were performed using AutoDock Vina v1.1.2. For each target protein, a grid box was centered on the reported active site or ligand-binding pocket; the grid box centers and dimensions are provided in Supplementary Table S1.

The docking parameters were set as follows: exhaustiveness = 8 and num\_modes = 10. The lowest binding energy pose for each ligand–protein complex was selected for further analysis. The selected poses were visualized and analyzed using PyMOL to identify hydrogen bonds and hydrophobic interactions, while two-dimensional interaction diagrams were generated using LigPlot+ [8].

Interpretation docking results are reported as exploratory, hypothesis-generating data and do not constitute proof of in vivo binding or pharmacological targeting.

## 2.8. Statistical Analysis

Data are presented as mean  $\pm$  SD. Normality was assessed using the Shapiro–Wilk test. For normally distributed data, comparisons among groups were performed by one-way ANOVA followed by Tukey's post hoc test; for non-normal data, Kruskal–Wallis with Dunn's post hoc test was used. Repeated measures (PASI over time) were analyzed by two-way ANOVA with repeated measures and Sidak's multiple comparisons test. Correlations were assessed by Pearson's correlation for normally distributed variables. A two-tailed  $p < 0.05$  was considered statistically significant. Analyses were performed using GraphPad Prism v9.0 [9].

# 3. Results

## 3.1. Clinical Scoring of Psoriasis-like Skin Manifestations

Erythema, induration (thickness), and scaling became macroscopically evident 2–3 days after the first topical application of imiquimod (IMQ). All three component scores and the composite murine PASI showed a progressive increase during the induction phase, reaching maximal values around day 8 (**Figure 1**, top and bottom panels). The negative control group maintained scores close to zero throughout the study, confirming intact skin at baseline and no spontaneous lesion development. In contrast, IMQ-treated animals exhibited a clear and reproducible rise in PASI scores that validated successful establishment of the psoriasis-like model.

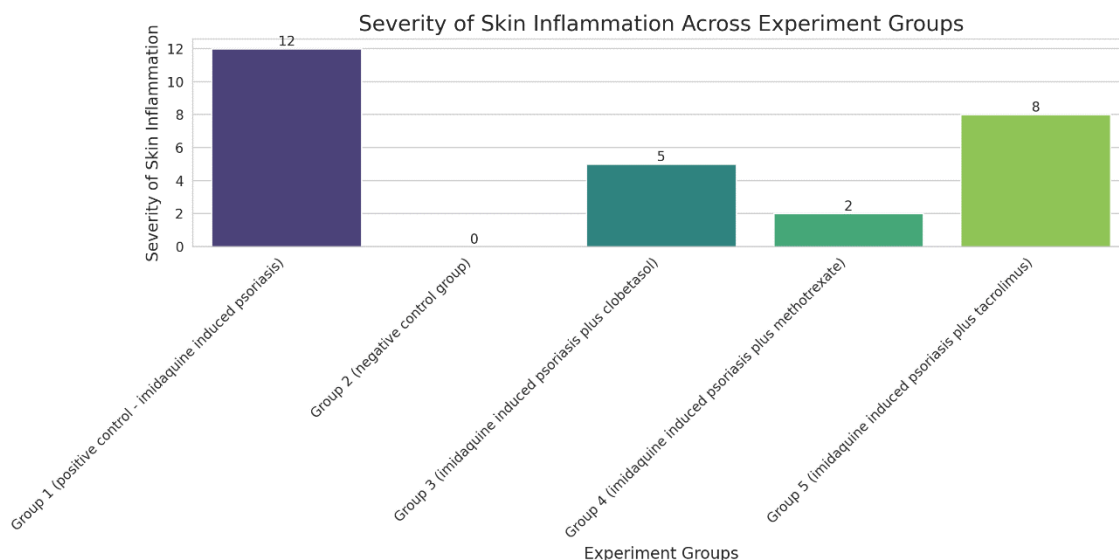


**Figure 1.** Severity of skin inflammation across experimental groups in a murine model of imiquimod-induced psoriasis.

One animal died during the acclimation/adaptation week; consequently, data for that mouse were excluded and the control group was not available for the day-2 assessment. All remaining animals completed the induction and treatment phases and were included in the analyses described below.

### 3.2. Time Course and Group Differences

PASI trajectories for the IMQ groups showed a rapid onset of inflammation (days 2–4), a peak around day 8, and a plateau or gradual change thereafter during the treatment period (**Figure 1**). The pattern was consistent across IMQ-only and IMQ + treatment groups, with differences in magnitude and temporal response apparent between treatment arms (see **Figure 1** and **Table 1** for group means ± SD and full statistical comparisons).

**Table 1.** Severity of Skin Inflammation among experimental groups (PASI score).

Experiment Groups	Severity of Skin Inflammation
Group 1 (positive control group—imiquimod-induced psoriasis)	12
Group 2 (negative control group)	0
Group 3 (imiquimod-induced psoriasis plus clobetasol)	5
Group 4 (imiquimod-induced psoriasis plus methotrexate)	2
Group 5 (imiquimod-induced psoriasis plus tacrolimus)	8

### 3.3. Validation of the Model

The divergence between the IMQ groups and the negative control in both component scores and total PASI confirms that the IMQ regimen produced a robust, reproducible inflammatory phenotype suitable for testing topical interventions. These clinical observations were corroborated by histopathological and biochemical endpoints (see Histology and Cytokine sections), which together support the validity of the model for evaluating topical anti-psoriatic effects.

### 3.4. The Histopathological Examination

The histopathological scoring system for all four groups was as follows: 0—normal skin; 1—mild inflammation, as evidenced by a sparse infiltrate of inflammatory cells, minimal tissue damage, and preservation of normal skin architecture; 2—moderate inflammation, as evidenced by a moderate infiltrate of inflammatory cells, moderate tissue damage, and partial disruption of normal skin architecture; 3—severe inflammation, as evidenced by a large infiltrate of inflammatory cells, significant tissue damage, and significant disruption of normal skin architecture; 4—most severe inflammation and tissue damage, as evidenced by extensive infiltrate of inflammatory cells, extensive disruption of normal skin architecture, and extensive tissue damage, as seen in the imiquimod-treated control group. The results were as follows: control negative—0; control positive—4; tacrolimus—3; clobetasol—2; methotrexate—1 (**Figure 2**: negative control; **Figure 3**:

positive control; **Figure 4** and **Figure 5**: tacrolimus group; **Figure 6**: clobetasol group; **Figure 7** and **Figure 8**: MTX group) [10].

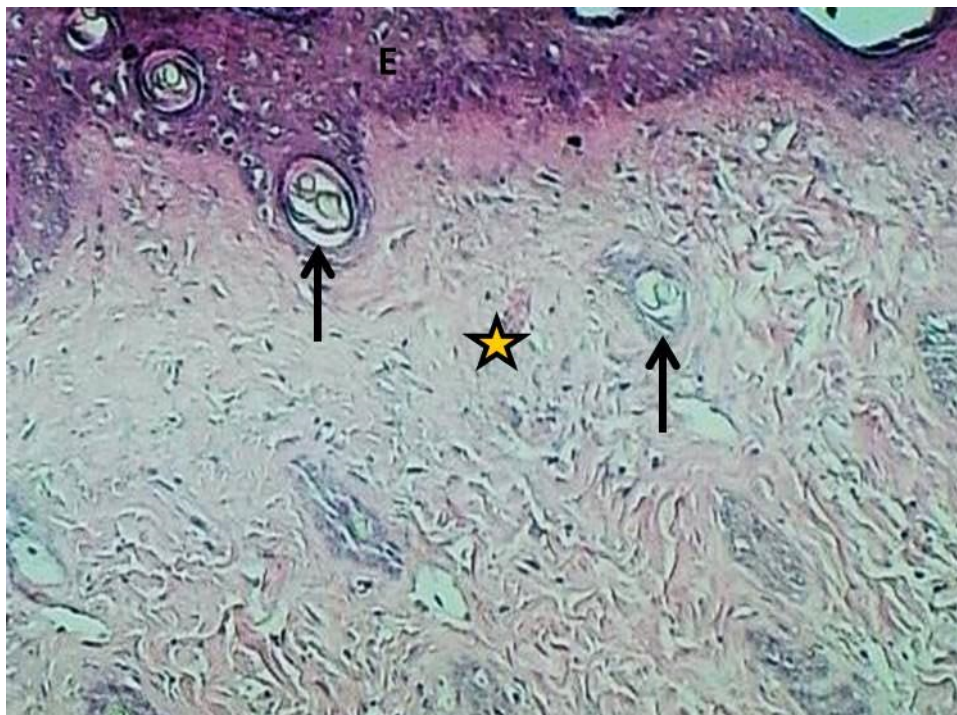


**Figure 2.** A biopsy section of the skin of the control negative group showing the normal structure of the epidermis, hair follicles, and dermal fibrous tissue. Hematoxylin and Eosin stain, 100 $\times$ . Scale bar = 100  $\mu$ m.

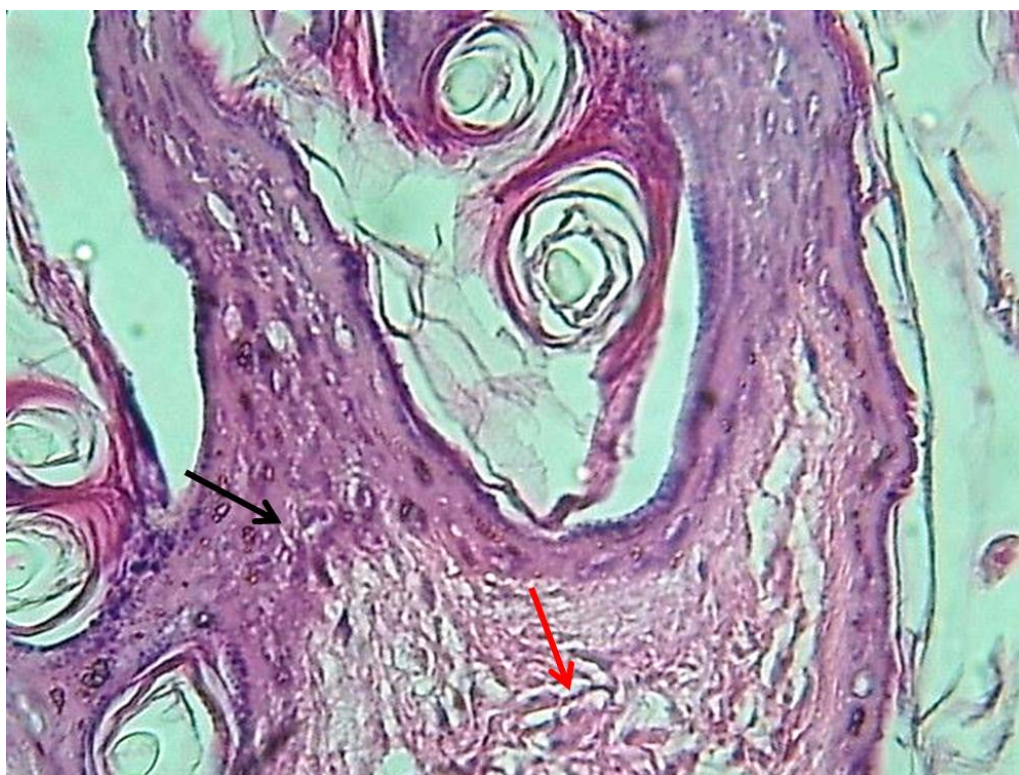


**Figure 3.** A biopsy section of the skin of the control positive group showing active mitotic figures in the basal cells of the epidermis, hair follicles, and dilated dermal capillaries. Hematoxylin and Eosin stain, 400 $\times$ . Scale bar = 25  $\mu$ m.

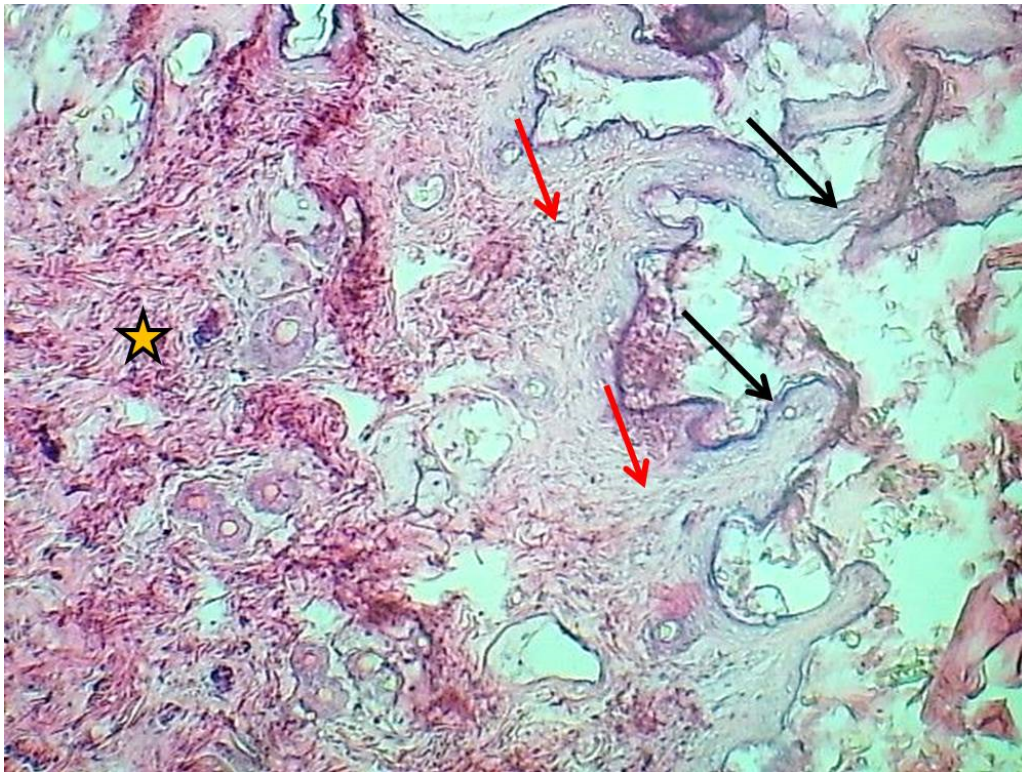


**Figure 4.** A biopsy section of the skin of the tacrolimus-treated group showing the pronounced irregular acanthosis of the epidermis, normal dermal fibrous tissue, and hair follicles. Hematoxylin and Eosin stain, 100 $\times$ . Scale bar = 100  $\mu$ m. Black arrow: irregular acanthosis of the epidermis; red arrow: hair follicle.

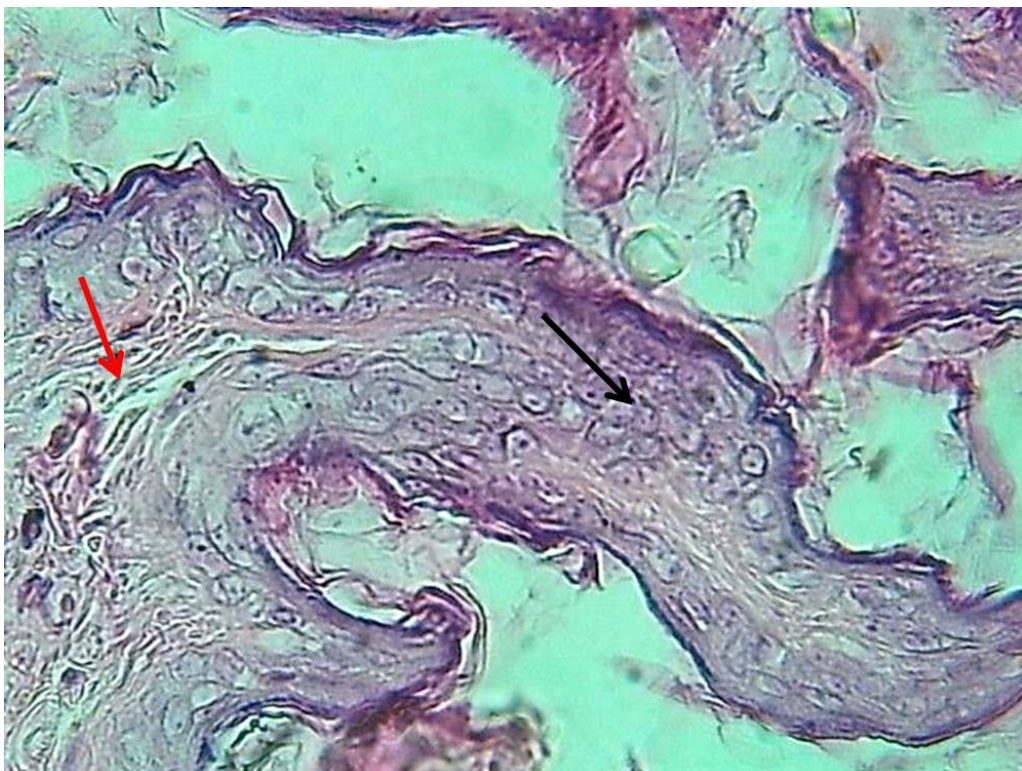


**Figure 5.** A biopsy section of the skin of the tacrolimus-treated group showing severe mitotic activity in the basal epithelial cells of the epidermis, the presence of an intact keratin layer, dermal fibrous tissue, and irregular acanthosis of the epidermis with the presence of hair follicles. Hematoxylin and Eosin stain, 400 $\times$ . Scale bar = 25  $\mu$ m. Red arrows: mitotic figures in basal epithelial cells; black arrow: hair follicle;  $\star$ : intact keratin layer (parakeratosis).

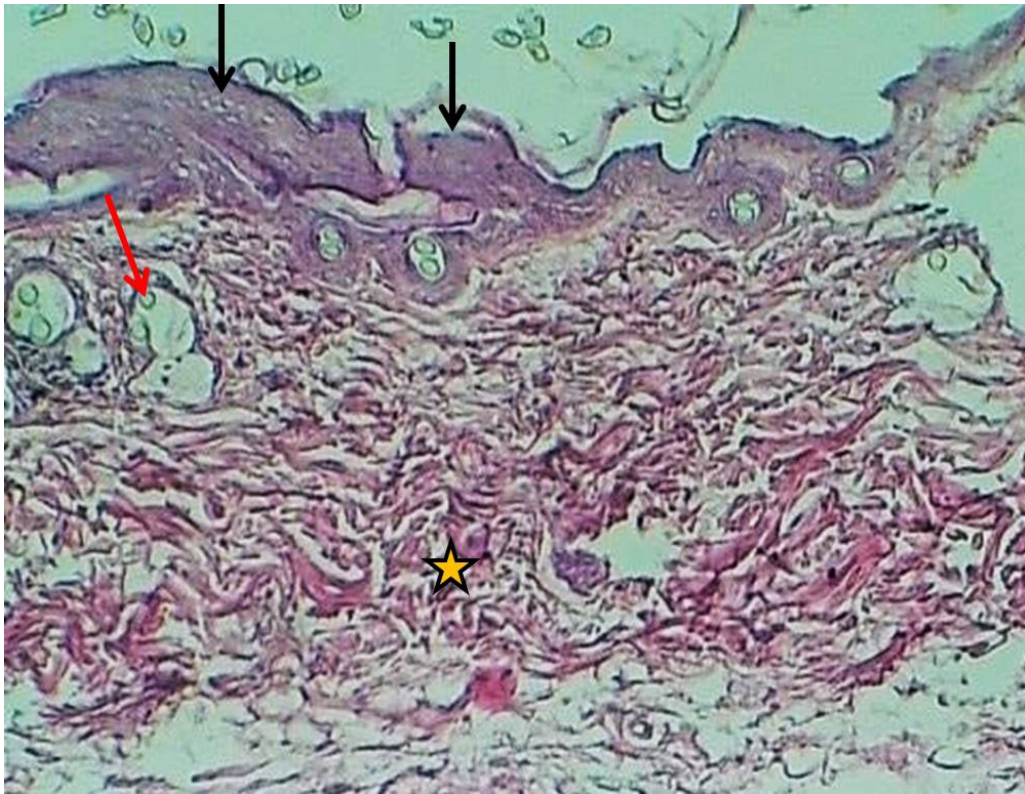


**Figure 6.** A biopsy section of the skin of the clobetasol propionate-treated group showing moderate irregular acanthosis of the epidermis, the presence of hair follicles, normal dermal fibrous tissue, and mature hair follicles with the presence of sebaceous glands. Hematoxylin and Eosin stain, 100 $\times$ . Scale bar = 100  $\mu$ m. Black arrow: moderate acanthosis of the epidermis; red arrow: mature hair follicle with sebaceous gland.

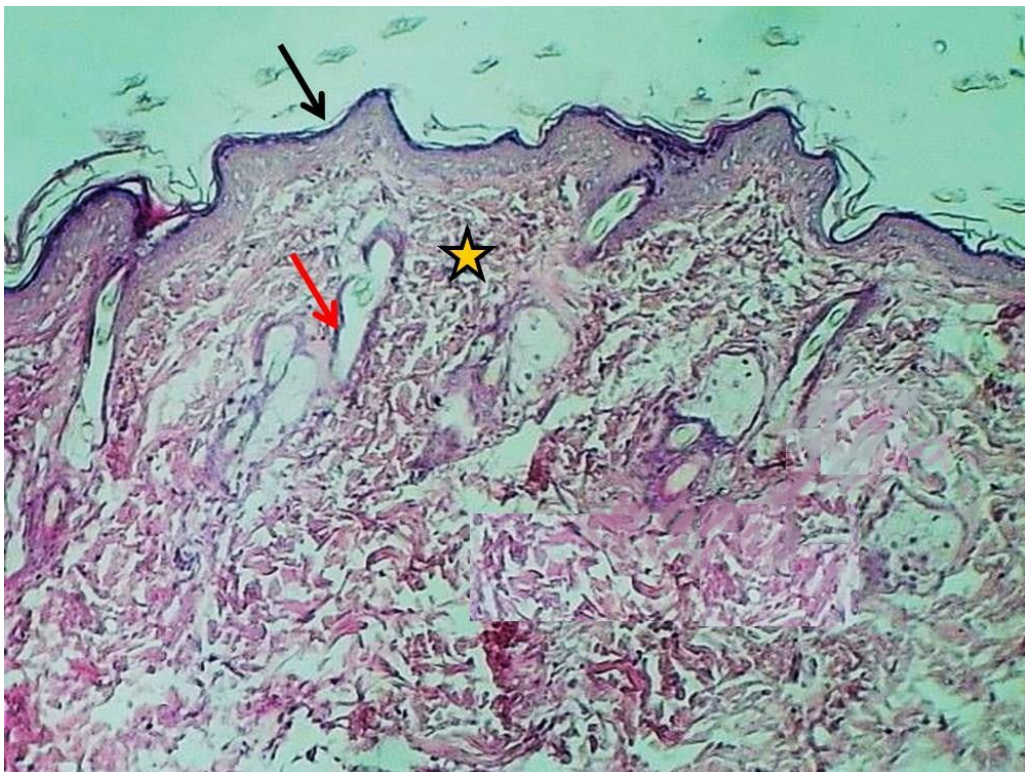


**Figure 7.** A biopsy section of the skin of the MTX-treated group showing normal epidermis, normal dermal fibrous tissue, and hair follicles. Hematoxylin and Eosin stain, 100 $\times$ . Scale bar = 100  $\mu$ m. Black arrow: normal epidermis; red arrow: hair follicle; arrowhead: dermal fibrous tissue.

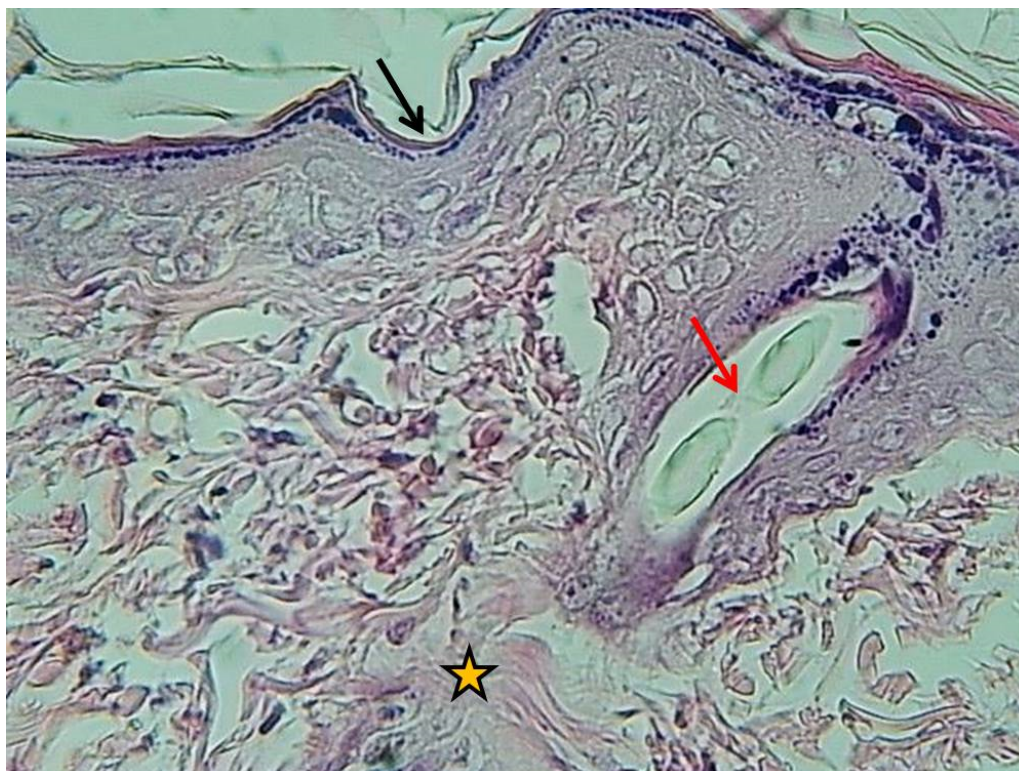


**Figure 8.** A biopsy section of the skin of the MTX-treated group showing normal epithelial cells of the epidermis, normal dermal fibrous tissue, and hair follicles. Hematoxylin and Eosin stain, 400×. Scale bar = 25 μm. Black arrow: normal stratified squamous epithelium; red arrow: hair follicle; arrowhead: dermal collagen (fibrous tissue).

### 3.5. Cytokines Results

Cytokine concentrations (TNF-α and IL-6) measured in skin tissue homogenates across all treatment groups are presented in **Table 2** and **Figure 9**. The positive control group showed significantly elevated TNF-α and IL-6 compared with negative controls, confirming successful model induction (**Table 2**). Treatment with clobetasol and topical MTX (1%) reduced both cytokines to near-baseline levels, while tacrolimus showed a significant reduction in TNF-α but not IL-6 ( $p = 0.060$ , ns).

**Table 2.** Cytokine levels (TNF-α and IL-6) across treatment groups.

Groups	TNF-Alpha pg/mg Protein (Mean ± SD)	IL-6 pg/mg Protein (Mean ± SD)	TNF-Alpha p-Value	IL-6 p-Value
Negative control	64.95 ± 5.94	35.086 ± 1.701	-	-
Positive control (vs. negative control)	124.32 ± 7.34	51.71 ± 4.39	$p = 0.001$	$p = 0.005$
GI (clobetasol-treated group)	77.79 ± 10.46	39.46 ± 4.43	$p = 0.020$	$p = 0.030$
GII (tacrolimus-treated group)	101.58 ± 7.15	45.14 ± 2.46	$p = 0.040$	$p = 0.060$ (ns)
GIII (mtx-treated group)	81.16 ± 7.34	38.83 ± 2.78	$p = 0.030$	$p = 0.020$

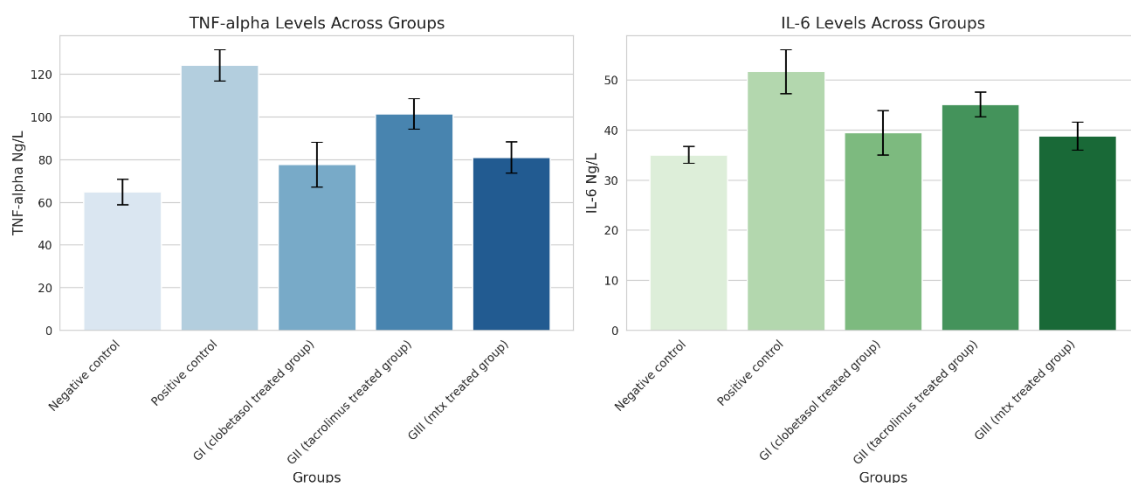


**Figure 9.** Cytokine levels (TNF-α and IL-6) in skin tissue homogenates across different treatment groups.

### 3.6. Clinical Course and Model Validation

Erythema, induration, and scaling were first evident 2–3 days after the initial topical IMQ application and increased progressively to a peak around day 8 (**Figure 1**). One mouse died during the acclimation week; data from that animal were excluded from all analyses. The negative control group maintained near-zero PASI scores throughout, confirming intact baseline skin, while IMQ treatment produced a reproducible psoriasis-like phenotype suitable for testing topical interventions.

For the Clobetasol-treated group, the cytokine levels of TNF-alpha and IL-6 are key findings.

- IMQ induction: The positive control group showed a robust pro-inflammatory response with significantly elevated TNF-α and IL-6 compared with negative controls (TNF-α  $p = 0.001$ ; IL-6  $p = 0.005$ ), confirming successful model induction.
- Clobetasol: Topical clobetasol significantly reduced both cytokines toward baseline (TNF-α  $p = 0.020$ ; IL-6  $p = 0.030$  versus negative control), consistent with potent anti-inflammatory activity.
- Tacrolimus: Tacrolimus produced a significant reduction in TNF-α ( $p = 0.040$ ) but the reduction in IL-6 did not reach statistical significance ( $p = 0.060$ ).
- Topical methotrexate (1%): MTX significantly lowered both TNF-α and IL-6 (TNF-α  $p = 0.030$ ; IL-6  $p = 0.020$  versus negative control) to values comparable with clobetasol. Pairwise comparison between MTX and clobetasol showed no significant difference for either cytokine ( $p > 0.05$ ), indicating similar efficacy in suppressing these inflammatory mediators in this model.

Interpretation IMQ produced a clear pro-inflammatory cytokine profile in skin. Both clobetasol and topical MTX (1%) effectively reduced TNF-α and IL-6 to near-baseline levels, while tacrolimus showed a more modest effect, significantly lowering TNF-α but not IL-6. These biochemical results align with the clinical PASI trajectories and histopathological improvements observed in the corresponding treatment groups (**Figure 9**; see **Figure 1** and histology results).

### 3.7. Molecular Docking Results

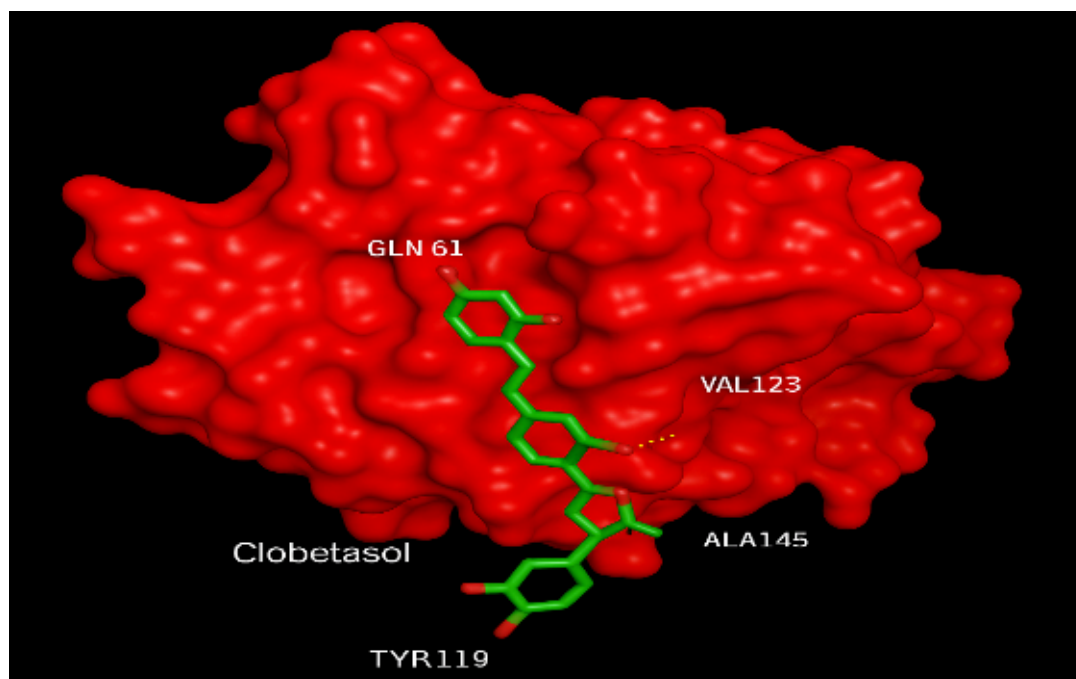
Molecular docking simulations were performed to study the interaction profiles of tacrolimus, methotrexate, and clobetasol propionate with TNF-α (PDB ID: 2AZ5) and IL-6 (PDB ID: 1IL6). The binding affinity values for top-ranked poses and key amino acid interactions are summarized in **Table 3** and **Table 4**; representative binding interactions are visualized in **Figure 10**.

**Table 3.** Molecular docking results of compounds with TNF-α (PDB ID: 2AZ5).

Compound	Binding Affinity (kcal/mol)	Key Interacting Residues
Tacrolimus	−9.1	TYR59, GLN61 (H-bonds); LEU120, VAL91, ALA145 (hydrophobic)
Clobetasol	−8.2	GLN61, TYR119 (H-bonds); LEU120, VAL123, ALA145 (hydrophobic)
Methotrexate	−7.6	SER60, TYR119, ASN92 (H-bonds); LEU120, VAL91 (hydrophobic)

**Table 4.** Molecular docking results of compounds with IL-6 (PDB ID: 1IL6).

Compound	Binding Affinity (kcal/mol)	Key Interacting Residues
Tacrolimus	−8.4	GLN75, ARG182 (H-bonds); LEU78, PHE74, VAL77, ILE175 (hydrophobic)
Clobetasol	−7.8	ARG179, GLN75 (H-bonds); LEU78, PHE74, VAL77 (hydrophobic)
Methotrexate	−7.4	ARG179, GLN75, ASN105 (H-bonds); LEU78, PHE74 (hydrophobic)

**Figure 10.** Molecular docking visualization of clobetasol bound to TNF- $\alpha$  (PDB ID: 2AZ5). Hydrogen bonding observed with GLN61 and TYR119.

## 4. Discussion

The present study evaluated the therapeutic potential of a 1% topical methotrexate (MTX) ointment in an imiquimod (IMQ)-induced murine model of psoriasis-like dermatitis. The IMQ model reproduced hallmark features of human psoriasis—epidermal hyperplasia, inflammatory cell infiltration, and a proinflammatory cytokine milieu dominated by TNF- $\alpha$  and IL-6—providing a relevant platform to compare topical MTX with established topical agents.

### 4.1. Efficacy: Clinical and Histological Outcomes

Topical MTX produced robust clinical improvement, reflected by significant reductions in PASI component scores (erythema, scaling, thickness) and by histological restoration toward normal epidermal architecture with decreased acanthosis and resolution of parakeratosis. These effects were comparable to clobetasol propionate (0.05%) and exceeded those observed with tacrolimus (0.1%) in this model. The histomorphological recovery observed with MTX—reduced epidermal proliferation and diminished inflammatory infiltrate—supports a direct antiproliferative effect on keratinocytes in addition to immunomodulation.

### 4.2. Cytokine Modulation and Mechanistic Considerations

Although the biomarker panel was limited to TNF- $\alpha$  and IL-6, these cytokines represent key mediators in psoriasis inflammation. Future studies should include additional markers such as IL-17 and IL-23 to better characterize the immunological pathways.

Biochemical analyses showed that topical MTX significantly lowered TNF- $\alpha$  and IL-6 levels in skin homogenates to values similar to those achieved with clobetasol. Mechanistically, these findings align with MTX's known actions as a folate antagonist that inhibits enzymes involved in nucleotide synthesis (e.g., DHFR, TYMS), thereby limiting proliferation of activated immune cells and hyperproliferative keratinocytes. MTX-mediated elevation of extracellular adenosine likely contributed to the observed suppression of proinflammatory cytokine production. The more modest effect of tacrolimus

on IL-6—despite a significant reduction in TNF- $\alpha$ —suggests differential downstream modulation of cytokine networks by calcineurin inhibition versus antifolate mechanisms [11].

### 4.3. In Silico Docking: Supportive but Exploratory Data

Docking simulations confirmed moderate predicted binding affinities of MTX, clobetasol, and tacrolimus to TNF- $\alpha$  and IL-6; these results should be interpreted cautiously as exploratory and not as evidence of direct cytokine antagonism *in vivo*. The combined *in vivo* and *in silico* data support a model in which topical MTX reduces cytokine levels primarily by acting on cellular sources (T cells, keratinocytes) and metabolic pathways rather than by direct blockade of soluble cytokines [12].

### 4.4. Comparison with Existing Literature and Formulation Considerations

Previous reports on topical MTX efficacy have been inconsistent, likely reflecting variability in vehicle composition, drug concentration, and skin penetration. The efficacy demonstrated here suggests that the chosen ointment base and 1% concentration achieved sufficient local bioavailability to exert therapeutic effects no safety assessment was performed in this preclinical setting. These results underscore the importance of formulation optimization (vehicle selection, penetration enhancers, particle size, and occlusion) when developing topical MTX products [13, 14].

## 5. Limitations

Key limitations temper the conclusions:

- Absence of pharmacokinetic and skin penetration data prevents definitive statements about local MTX concentrations and systemic exposure.
- Cytokine panel was limited to TNF- $\alpha$  and IL-6; the IL-23/IL-17 axis—central to psoriasis pathogenesis—was not quantified and should be included in follow-up studies.
- Single concentration and vehicle were tested; dose–response relationships and alternative vehicles were not explored.
- Translatability from murine IMQ models to human psoriasis is imperfect; clinical trials are required to confirm safety and efficacy in patients.
- Histological quantification could be strengthened by additional objective morphometric endpoints and blinded digital image analysis across larger sampling fields.

## 6. Future Directions

Future work should: (1) include skin pharmacokinetics and systemic exposure measurements to confirm localized action and safety; (2) expand cytokine and cellular profiling to encompass the IL-23/IL-17 axis and immune cell phenotyping; (3) evaluate dose–response and alternative formulation strategies (e.g., liposomal, nanoemulsion, or microneedle-assisted delivery) to optimize penetration and minimize systemic absorption; and (4) progress to well-designed clinical studies if preclinical safety and pharmacokinetic data support translation.

## 7. Conclusion

This study provides proof-of-concept that a 1% topical MTX ointment can produce clinically and histologically meaningful improvement in an IMQ-induced psoriasis-like model, with cytokine suppression comparable to a potent topical corticosteroid. Topical MTX merits further preclinical optimization and pharmacokinetic evaluation as a potential steroid-sparing topical therapy for localized psoriatic lesions.

## Acknowledgments

The author thanks the Center for Biotechnology, Al-Nahrain University, for providing laboratory facilities and equipment used in this study.

## Funding

This research received no external funding.

## Author contributions

Conceptualization, M.A.M.A.B.; methodology, M.A.M.A.B.; software, M.A.M.A.B.; formal analysis, M.A.M.A.B.; investigation, M.A.M.A.B.; resources, M.A.M.A.B.; data curation, M.A.M.A.B.; writing—original draft preparation, M.A.M.A.B.; writing—review and editing, M.A.M.A.B.; visualization, M.A.M.A.B. The author has read and agreed to the published version of the manuscript.

## Conflicts of interest

The author declares no conflicts of interest.

## Data availability statement

The data presented in this study are available upon reasonable request from the corresponding author.

## Institutional review board statement

The animal study protocol was conducted in accordance with internationally accepted guidelines (ARRIVE guidelines) and was approved by the Institutional Animal Care and Use Committee of the Center for Biotechnology, Al-Nahrain University, Baghdad, Iraq.

## Informed consent statement

Not applicable. This study involved animals only.

## Supplementary materials

The supplementary materials are available at <https://doi.org/10.6425/042026jept005>. Table S1. *Grid box center coordinates and dimensions used for AutoDock Vina molecular docking simulations against the six target proteins (DHFR, PDB 1U72; TYMS, PDB 1HVY; ATIC, PDB 1D3G; DHODH, PDB 6QU7; TNF- $\alpha$ , PDB 2AZ5; IL-6, PDB 1IL6), including the x, y, z grid center coordinates and the box dimensions (Å) applied for each ligand–target docking run.*

## Additional information

Received: 2026-03-22

Accepted: 2026-05-13

Published: 2026-07-01

## Publisher's note

The Journal of Experimental Pharmacology and Toxicology remains neutral with regard to jurisdictional claims in published maps and institutional affiliations. All claims expressed in this article are solely those of the authors and do not necessarily represent those of their affiliated organizations, or those of the publisher, the editors, and the reviewers. Any product that may be evaluated in this article, or claim that may be made by its manufacturer, is not guaranteed or endorsed by the publisher.

## Copyright

© 2026 copyright by the author. This article is an open access article distributed under the terms and conditions of the Creative Commons Attribution (CC BY) license (<https://creativecommons.org/licenses/by/4.0/>).

## References

1. Fraillon E. Comparative analysis of cutaneous features of psoriasis-like inflammation in IMQ murine models. *Sci Rep.* 2025; 15: 27634. doi: 10.1038/s41598-025-27634-0
2. AlQarqaz F. Advances in systemic and topical treatments for severe psoriasis: an updated review. *Clin Cosmet Investig Dermatol.* 2023; 16: 1923–37. doi: 10.2147/CCID.S416655
3. Ashraf I. Updated guidelines for the safe and effective use of methotrexate in dermatology. *J Dermatolog Treat.* 2023; 34 (1): 2151849. doi: 10.1080/09546634.2022.2151849
4. Sezer Z, İnal A, Çınar SL, Mazıcioğlu MM, Altuğ S, Karasulu HY, et al. Safety and efficacy of a novel combination cream (GN-037) in healthy volunteers and patients with plaque psoriasis: a phase 1 trial. *Dermatol Ther (Heidelb).* 2023; 13 (7): 1489–501. doi: 10.1007/s13555-023-00953-5
5. Lim Y, Park SH, Kim EJ, Lim H, Jang J, Hong I, et al. Polar microalgae extracts protect human HaCaT keratinocytes from damaging stimuli and ameliorate psoriatic skin inflammation in mice. *Biol Res.* 2023; 56 (1): 40. doi: 10.1186/s40659-023-00454-5

6. Dyring-Andersen B, Løvendorf MB, Coscia F, Santos A, Møller LBP, Colaço AR, et al. Spatially and cell-type resolved quantitative proteomic atlas of healthy human skin. *Nat Commun.* 2020; 11 (1): 5587. doi: 10.1038/s41467-020-19383-8
7. Al-Robai SA, Ahmed AA, Ahmed AAE, Zabin SA, Mohamed HA, Alghamdi AAA. Phenols, antioxidant and anticancer properties of *Tagetes minuta*, *Euphorbia granulata* and *Galinsoga parviflora*: in vitro and in silico evaluation. *J Umm Al-Qura Univ Appl Sci.* 2022; 9 (1): 15–28. doi: 10.1007/s43994-022-00013-w
8. Dahiru MM, Musa N, Abaka AM, Abubakar MA. Potential antidiabetic compounds from *Anogeissus leiocarpus*: molecular docking, molecular dynamic simulation, and ADMET studies. *Borneo J Pharm.* 2023; 6 (3): 249–77. doi: 10.33084/bjop.v6i3.4693
9. Juczewski K, Koussa JA, Kesner AJ, Lee JO, Lovinger DM. Stress and behavioral correlates in the head-fixed method: stress measurements, habituation dynamics, locomotion, and motor-skill learning in mice. *Sci Rep.* 2020; 10 (1): 12191. doi: 10.1038/s41598-020-68999-x
10. Mohammed S, Kadhim HM, AL-Sudani IM, Musatafa WW. Anti-inflammatory effects of topically applied azilsartan in a mouse model of imiquimod-induced psoriasis. *Int J Drug Deliv Technol.* 2022; 12 (3): 1249–55. doi: 10.25258/ijddt.12.3.32
11. Traitanon O, Mathew JM, Monica GL, Xu L, Mas VR, Gallon L. Differential effects of tacrolimus versus sirolimus on the proliferation, activation and differentiation of human B cells. *PLoS ONE.* 2015; 10 (6): e0129658. doi: 10.1371/journal.pone.0129658
12. Chaiyabutr C, Punnakitikashem P, Silpa-archa N, Wongpraparut C, Chularojanamontri L. The anti-psoriatic efficacy and safety profile of topical and intralesional methotrexate: a literature review. *Clin Cosmet Investig Dermatol.* 2022; 15: 2253–74. doi: 10.2147/CCID.S386800
13. Veer PJ, Mastiholimath VS. Formulation, characterization, and optimization of transethosomes for enhanced transdermal delivery of methotrexate. *J Pharm Innov.* 2023; 18 (4): 2385–401. doi: 10.1007/s12247-023-09760-x
14. Das T, Prakash M, Kumar P. Injectable in situ gel of methotrexate for rheumatoid arthritis: development, in vitro and in vivo evaluation. *J Appl Pharm Sci.* 2019; 9 (5): 40–48. doi: 10.7324/JAPS.2019.90505